ELSEVIER

Materials Science and Engineering A267 (1999) 220–226

MATERIALS SCIENCE & ENGINEERING A

CO_2 methanation catalysts prepared from amorphous Ni–Zr–Sm and Ni–Zr–misch metal alloy precursors

Michiaki Yamasaki [a,*], Mitsuru Komori [b], Eiji Akiyama [a], Hiroki Habazaki [a], Asahi Kawashima [a], Katsuhiko Asami [a], Koji Hashimoto [a]

[a] *Institute for Materials Research, Tohoku University, Sendai 980-8577, Japan*
[b] *Ryoka Matthey Corporation, 1 Fukuda, Joetsu, Niigata 942-8611, Japan*

Abstract

Nickel catalysts supported on nano-grained oxides have been prepared from amorphous Ni–Zr–Sm and Ni–Zr–Mm (Mm: misch metal) alloys and crystalline Ni–Sm and Ni–Mm alloys. These catalysts show higher catalytic activity for methanation of carbon dioxide than a conventionally prepared zirconia supported nickel catalyst. The catalytic activity of Ni–Zr–5 at% Sm catalysts increases with increase in nickel content, and is higher than the samarium-free Ni–Zr catalysts containing the same amount of nickel. The stabilization of tetragonal zirconia and the increase in the number of active surface nickel sites by addition of samarium to the nickel-rich catalysts leads to enhancement of catalytic activity. In the Ni–Zr–5 at% Mm catalysts, only the activity of the catalyst containing 60 at% nickel is enhanced in comparison with misch metal-free Ni–Zr catalysts. It is also found that Ni–Sm and Ni–Mm catalysts show activities as high as that of Ni–Zr catalyst, suggesting that samarium and misch metal oxides also act as good catalyst supports for methanation catalysts. © 1999 Elsevier Science S.A. All rights reserved.

Keywords: Amorphous alloy precursors; Nickel catalysts; Tetragonal zirconia; Carbon dioxide; Methanation; Samarium

1. Introduction

In recent years, global warming has been discussed in all sorts of fields. On this occasion, the third session of the conference of the parties to the United Nations Framework Convention on Climate Change (COP3) was held in Kyoto in December 1997. The results of settlement brought to a conclusion as 'Kyoto protocol to the United Nations Framework Convention on Climate Change'. Consequently, every participating nation has definite curtailment targets for greenhouse gases according to each country's ability.

Global warming caused by enormous evolution of carbon dioxide by combustion of fossil fuels has become a serious problem in industrial circles. In order to solve this problem, various types of methods for recovering and chemical fixation of carbon dioxide have been proposed. Methanation of carbon dioxide is the most advantageous reaction with respect to thermodynamics for chemical fixation of carbon dioxide, since the reaction is considerably faster than reactions to form other hydrocarbons or alcohols [1]. The present authors are proposing global carbon dioxide recycling [2], which consists of generating electricity in deserts, producing hydrogen and methane on coasts close to the deserts and using methane as the energy source on consumer locations. In the deserts, electricity is generated by solar cells. On coasts close to the deserts, the electricity is used for hydrogen production by electrolysis of seawater, and methane is formed by the reaction of the hydrogen with carbon dioxide and sent to energy consumers. Energy consumers, after using methane as a fuel, recover and send carbon dioxide to the coasts close to the deserts. A carbon dioxide recycling plant for substantiation of our idea has been built in 1996 on the roof of our Institute using novel materials tailored by us, such as electrodes for seawater electrolysis [3,4] and amorphous alloy catalysts for methanation of carbon dioxide [5,6]. The development of catalysts for methanation of carbon dioxide was the key factor.

Amorphous alloys are interesting materials for novel catalysts and catalyst precursors since it is possible to

* Corresponding author. Tel.: +81-22-2152082; fax: +81-22-2152081.
E-mail address: yamasaki@imr.tohoku.ac.jp (M. Yamasaki)

0921-5093/99/$ - see front matter © 1999 Elsevier Science S.A. All rights reserved.
PII: S0921-5093(99)00095-7

improve the electronic states of active elements and produce synergistic effects by alloying with various elements. One of the advantages of amorphous alloys is the possibility of forming single solid solutions with compositions far exceeding the solubility limits in the equilibrium state. In fact, there are several reports to show that amorphous alloys have extremely high catalytic activity and high selectivity for some reactions.

Komiyama et al. reported that amorphous Fe–Ni–P–B alloy catalysts show catalytic activity for hydrogenation of carbon monoxide about 200 times higher than those of the corresponding crystalline counterparts [7,8]. They concluded that the activity is due to high density of the active site in the amorphous alloy catalysts. Yokoyama et al. have found that the activity for methanation of carbon monoxide on amorphous Pd–Zr alloys increases with reaction time by in situ activation [9]. They considered that the activation is due to the formation of an active complex oxide consisting of Pd–Zr–O from amorphous Pd–Zr alloy precursors. Takahashi et al. [10] have also reported that amorphous Pd–Zr alloys become highly active catalysts for hydrogenation of benzene by oxidation and subsequent reduction. From that time, amorphous alloys have received much attention as catalyst precursors. For example, Molnár et al. have reported on catalysts formed from amorphous copper-valve metal alloy precursors for dehydrogenation of 2-propanol [11–16]. By various pretreatments, the alloys are converted to active catalysts consisting of copper supported on valve metal oxides. The catalysts prepared from amorphous Cu–Zr [17], Pd–Zr [18] and Rh–Zr [19] alloys for hydrogenation of carbon dioxide have also been reported.

In our studies [5], it was found that the catalysts prepared from amorphous Ni–Zr binary alloys show the highest activity for methanation of carbon dioxide among various amorphous binary alloys consisting of iron group elements and valve metal elements. The reaction equation of methanation of carbon dioxide is as follows.

$$CO_2 + 4H_2 = CH_4 + 2H_2O$$

$$\Delta G^0_{298} = -113.6 \text{ kJ mol}^{-1}$$

In the atmosphere under the reaction, nickel remains in the metallic state, but zirconium is oxidized to zirconia. Namely, during the reaction, amorphous Ni–Zr alloys are converted to zirconia supported nickel catalysts. The stable form of zirconia at room temperature is the monoclinic phase. However, in these catalysts, two types of zirconia are present, namely monoclinic and tetragonal phases [6]. The relative peak intensity of the tetragonal phase in the X-ray diffraction patterns increases gradually with increasing nickel content in the catalysts. The metastable tetragonal phase is stabilized by the formation of nano-grained zirconia [20–22] and by the dissolution of nickel in zirconia. The turnover number of the catalysts also increases gradually with increasing nickel content. Accordingly, there is a good correlation between the turnover number and the amount of tetragonal zirconia. Therefore, the nickel supported on the tetragonal zirconia has higher activity than that supported on monoclinic zirconia [23]. Furthermore, the addition of rare earth elements to amorphous Ni–Zr alloys is effective in enhancing the activity for methanation of carbon dioxide [24,25]. Samarium containing catalysts have the highest activity in comparison with cerium and yttrium containing [25] catalysts. The present work aims to clarify the beneficial effect of samarium addition in comparison with that of a mixture of rare earth elements, that is, misch metal.

2. Experimental

2.1. Catalyst preparation

Crystalline alloy ingots were prepared by argon arc melting of 99.95% pure nickel, 99.6% pure zirconium and 99.9% pure samarium or misch metal (a mixture of rare earth elements, La: 22.76 at%, Ce: 54.40 at%, Pr: 5.97 at%, Nd: 16.87 at%). Amorphous alloy ribbons of about 1 mm width and 30 μm thickness were formed by a single roller melt-spinning method in an argon atmosphere. The amorphous structure was confirmed by X-ray diffraction using Cu Kα radiation. Fig. 1 shows the composition-structure diagram of amorphous Ni–Zr–Sm and Ni–Zr–Mm (Mm: misch metal) respectively. Prior to catalytic reactions, the amorphous alloys thus prepared were oxidized in air at 773 K for 5 h and subsequently reduced under hydrogen flow at 573 K for at least 5 h.

A 3 at% nickel catalyst supported on zirconia was prepared by a wet impregnation method. Commercial zirconia was impregnated with a solution of $Ni(NO_3)_2$, and then dried at 373 K for 20 h. After calcination in

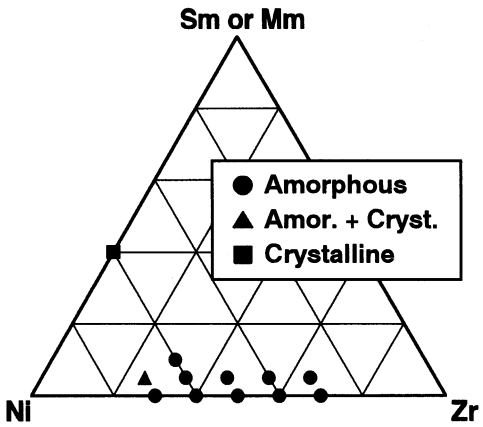

Fig. 1. A composition-structure diagram of Ni–Zr–Sm and Ni–Zr–Mm alloy catalyst precursors.

air at 723 K for 2 h and subsequent reduction under hydrogen flow at 573 K, the specimen was used as a conventionally supported catalyst for methanation of carbon dioxide.

2.2. Catalytic reaction

The catalytic reaction was performed in a continuous tubular flow reactor of 15 mm inner diameter under atmospheric pressure. The reaction gas mixture of CO_2 and H_2 (1:4 volume ratio) was passed continuously through the catalyst with $F/W = 1.5$ ml g^{-1} s^{-1}. After the reaction, the gas mixture was analyzed using a Chrompac MicroGC CP2002 gas chromatograph equipped with a thermal conductivity detector. The catalytic reaction was performed at temperatures ranging from 423 to 623 K. The turnover number of the catalysts was determined using a differential reactor and the number of surface nickel atoms was determined by hydrogen chemisorption measurements.

2.3. Catalyst characterization

Nitrogen physisorption and hydrogen chemisorption measurements were carried out at 77 and 293 K, respectively, with a Belsorp 28SA automatic gas adsorption apparatus. Prior to the measurement, the catalysts were reduced under hydrogen flow at 573 K for 2 h and then the chamber was evacuated and kept at the same temperature for 3 h. Hydrogen uptake at 293 K was calculated by extrapolating the linear part of the hydrogen adsorption isotherm to zero pressure. The isotherm was obtained from the difference of the first and second runs of the isotherm measurement in order to remove the contribution of hydrogen physisorption. Nickel particle sizes in the catalysts were estimated assuming spherical particles.

The structure of catalysts was determined by X-ray diffraction using Cu Kα radiation and the morphologies of the specimen cross-sections were observed by scanning electron microscopy (SEM) equipped with energy dispersive X-ray spectrometer (EDX).

3. Results and discussion

3.1. Catalytic activity

Fig. 2 shows the conversion of carbon dioxide at several temperatures on the Ni–Zr–5 at% Sm catalysts as a function of precursor alloy composition. At 573 K, the 90% conversion of carbon dioxide is reached on most of the catalysts. At 523 K, the conversion decreases abruptly with a decrease in nickel content from 40 to 30 at% in the precursor alloys. At 473 K, an increase in nickel content leads to a gradual increase in the catalytic activity, in comparison with the samarium-free Ni–Zr catalysts which show the highest conversion on the catalyst with 50 at% nickel. The Ni–25Zr–5Sm catalyst reveals the highest activity of all the catalysts examined. Fig. 3 shows the conversion of carbon dioxide at several temperatures on the Ni–Zr–5 at% Mm catalysts as a function of precursor alloy composition. Only the activity of the catalyst with 60 at% nickel was enhanced by the addition of misch metal, in comparison with the misch metal-free Ni–Zr catalysts at 473 K.

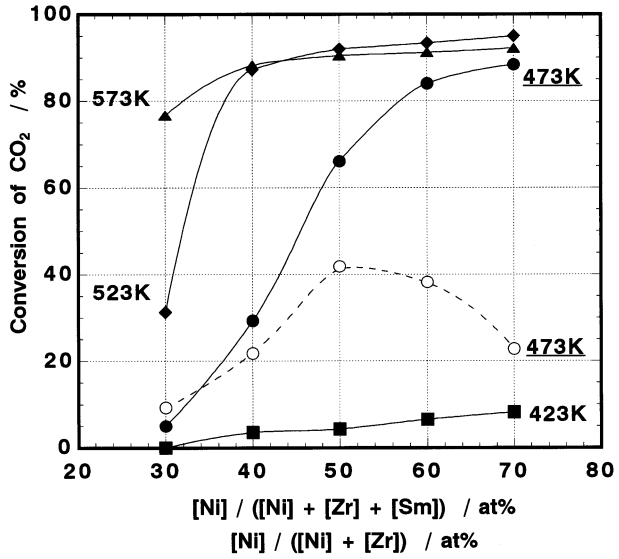

Fig. 2. The conversion of carbon dioxide on the catalysts prepared from the amorphous Ni–Zr–5 at% Sm (solid symbols) and Ni–Zr (open symbols) alloy precursors as a function of nickel content in precursor alloys. $F/W = 1.5$ ml g^{-1} s^{-1}, $H_2/CO_2 = 4$.

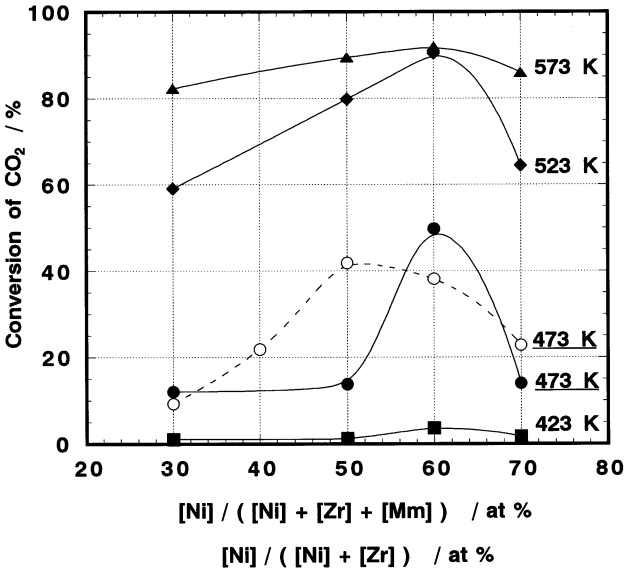

Fig. 3. The conversion of carbon dioxide on the catalysts prepared from the amorphous Ni–Zr–5 at% Mm (solid symbols) and Ni–Zr (open symbols) alloy precursors as a function of nickel content of precursor alloys. $F/W = 1.5$ ml g^{-1} s^{-1}, $H_2/CO_2 = 4$.

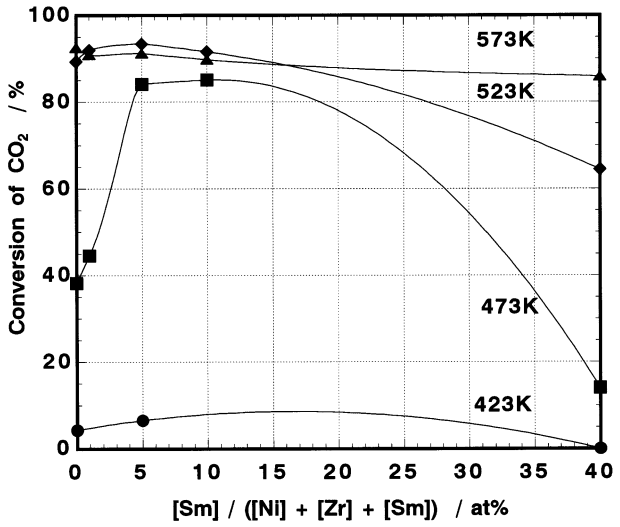

Fig. 4. Change in the conversion of carbon dioxide on the catalysts prepared from the amorphous and crystalline 60 at% Ni–$(40-x)$ at% Zr – x at% Sm alloy precursors as a function of nickel content of precursor alloys. $F/W = 1.5$ ml g^{-1} s^{-1}, $H_2/CO_2 = 4$.

Figs. 4 and 5 show the conversion of carbon dioxide on the catalysts containing 60 at% nickel and different concentrations of samarium and misch metal, respectively. At higher and lower reaction temperatures, the effects of the addition of rare earth elements are not clear and the additions of 5–10 at% of samarium and misch metal are effective at enhancing the catalytic activity only at 473 K. The samarium addition is more effective than the misch metal addition. The higher catalytic activity appears at 5 at% misch metal.

A comparison among zirconium, samarium and misch metal supports is given in Fig. 6 which shows the

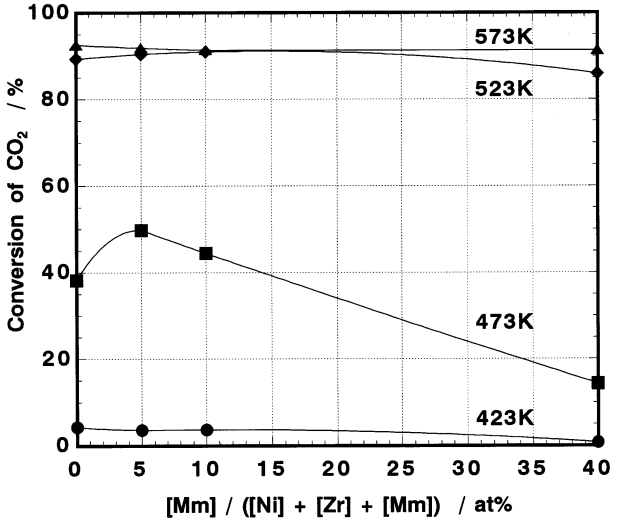

Fig. 5. Change in the conversion of carbon dioxide on the catalysts prepared from the amorphous and crystalline 60 at% Ni–$(40-x)$ at% Zr – x at% Mm alloy precursors as a function of nickel content of precursor alloys. $F/W = 1.5$ ml g^{-1} s^{-1}, $H_2/CO_2 = 4$.

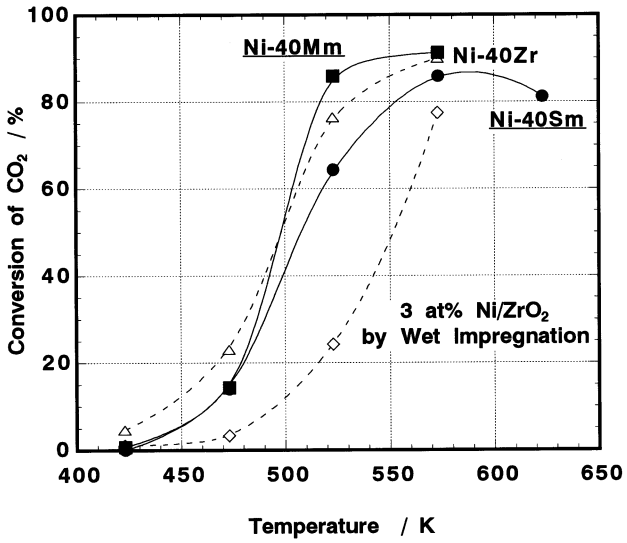

Fig. 6. Temperature dependence of the conversion of carbon dioxide on the catalysts prepared from the amorphous Ni–40 at% Zr and crystalline Ni–40 at% Sm and Ni–40 at% Mm alloy precursors and on the catalyst prepared by wet impregnation. $F/W = 1.5$ ml g^{-1} s^{-1}, $H_2/CO_2 = 4$.

temperature dependence of the conversion of carbon dioxide on catalysts prepared from the amorphous Ni–40Zr alloy, the crystalline Ni–40Sm and Ni–40Mm alloys and the one prepared by wet impregnation. The activities of the Ni–40Sm and Ni–40Mm catalysts are higher than that of the catalyst prepared by wet impregnation and are as high as that of the Ni–40Zr catalyst. Accordingly, samarium oxide and misch metal oxide are regarded as good supports of the catalyst for methanation of carbon dioxide. In these experiments, methane selectivity on all the catalysts was practically 100%.

3.2. Characterization of catalysts

To clarify the role of samarium, X-ray diffraction analysis was carried out for Ni–25Zr–5Sm, Ni–45Zr–5Sm, Ni–65Zr–5Sm and Ni–50Zr catalysts after the reaction. The results are shown in Fig. 7. Two types of zirconia were identified in the Ni–50Zr catalyst, that is, tetragonal and monoclinic zirconia. It is noteworthy that reflections of tetragonal zirconia are more diffuse than those of monoclinic zirconia. This indicates that the grain size of the tetragonal zirconia is smaller than that of the monoclinic zirconia. In the Ni–45Zr–5Sm catalyst, tetragonal zirconia was predominantly formed. The Ni–25Zr–5Sm catalyst also has only tetragonal zirconia. By contrast, in the Ni–65Zr–5Sm catalyst, monoclinic zirconia was mainly present. Fig. 8 shows the relative peak height of the 111 reflection for tetragonal zirconia at the diffraction angle of about 30°, with respect to the total peak heights of the 111 reflection for

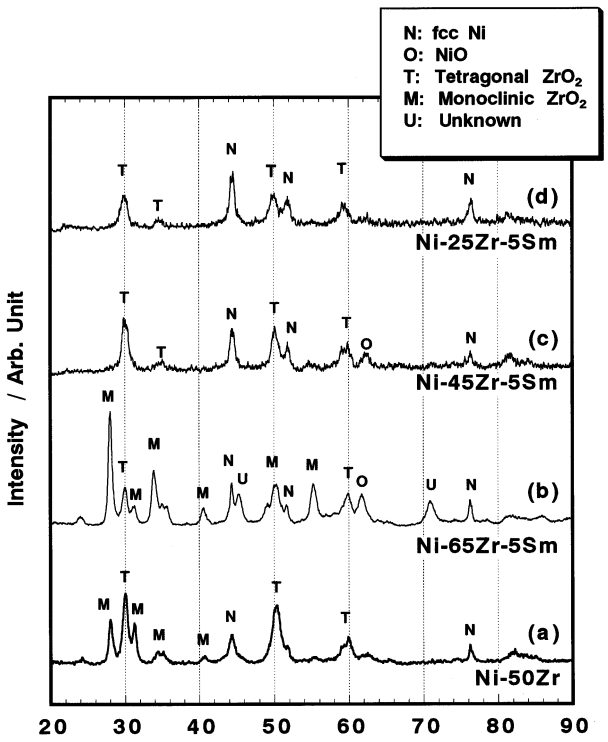

Fig. 7. X-Ray diffraction patterns of the catalysts prepared from the amorphous Ni–50 at% Zr and Ni–Zr–5 at% Sm alloy precursors.

tetragonal zirconia and the $\bar{1}11$ reflection for monoclinic zirconia at the diffraction angle of about 28°, as a function of nickel content. Except for Ni–65Zr–5Sm alloy, the tetragonal zirconia is exclusively formed from

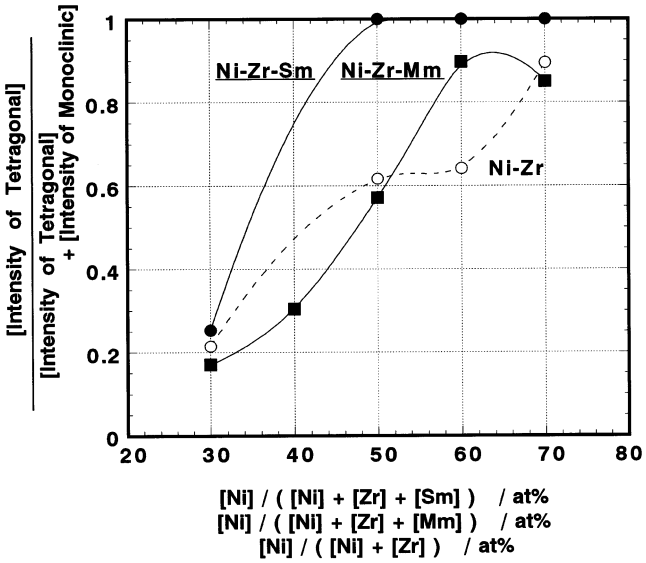

Fig. 8. Change in the relative peak height of 111 reflection for the tetragonal zirconia, with respect to the sum of the peak heights of 111 reflection for the tetragonal zirconia and $\bar{1}11$ reflection for the monoclinic zirconia in the catalysts prepared from the amorphous Ni–Zr, Ni–Zr–Sm and Ni–Zr–Mm alloy precursors as a function of nickel content in the alloy precursors.

Table 1
BET surface area on the catalysts prepared from the amorphous Ni–Zr and Ni–Zr–Sm alloy precursors

Specimen	BET surface area ($m^2\ g^{-1}$)
Ni–30Zr	6.8
Ni–25Zr–5Sm	19.8
Ni–40Zr	8.7
Ni–35Zr–5Sm	14.9
Ni–50Zr	7.4
Ni–45Zr–5Sm	13.4

samarium-containing alloys. The stabilization of the tetragonal zirconia by samarium addition should be one of the reasons for the high activity of samarium containing Ni–Zr catalysts. If the nickel content is adequate, that is 60 at%, the addition of misch metal is also effective to stabilize the tetragonal zirconia. Enhancement of catalytic activity depends on the relative amount of tetragonal zirconia as can be seen in Figs. 2 and 3. The results from Figs. 6 and 2 suggest that the activity of catalysts for methanation of carbon dioxide increases in the following order of oxide supports: monoclinic zirconia, samarium oxide, misch metal oxide and tetragonal zirconia.

BET surface areas were calculated from the results of nitrogen physisorption measurements. Table 1 shows BET surface areas of Ni–Zr catalysts and Ni–Zr–5 at% Sm catalysts. BET surface areas increase with increasing nickel content in the samarium containing catalysts and the samarium addition increases the roughness. The hydrogen chemisorption takes place on the surface nickel atom [26] and thus, an increase in hydrogen uptake indicates an increase in the number of surface nickel atoms, that is, the active sites for methanation of carbon dioxide. The results of hydrogen chemisorption measurements are summarized in Table 2. The addition of samarium increases the number of surface nickel atoms in nickel-rich catalysts and hence, samarium addition enhances the dispersion of nickel. However, in zirconium-rich catalysts, hydrogen uptake of samarium-containing catalysts is lower than that of samarium-free Ni–Zr catalysts. Thus, the number of active sites, that is, surface nickel atoms, also decreases. Barrault and Chafik [27] reported that the addition of a few percent of lanthanum, cerium and samarium to carbon supported nickel catalysts is effective in dispersing nickel atoms. Furthermore, as can be seen in Fig. 9, the turnover number of the samarium containing catalyst is higher than that of the samarium-free catalyst and increases with nickel content due to the stabilization of tetragonal zirconia. Because of the stabilization of tetragonal zirconia and because of an increase in the number of surface nickel atoms, the nickel-rich catalysts containing samarium show extremely high activity for methanation of carbon dioxide.

Table 2
Summary of hydrogen chemisorption on the catalysts prepared from amorphous Ni–Zr and Ni–Zr–Sm alloys and by wet impregnation

Specimen	H_2 uptake (ml g^{-1})	Number of surface nickel atoms ($\times 10^{19}$ atoms)	Nickel particle size (nm)	Metal dispersion (%)
Ni–30Zr	0.63	3.39	85.0	0.63
Ni–25Zr–5Sm	1.93	10.37	20.9	2.2
Ni–40Zr	1.19	6.37	28.4	1.5
Ni–35Zr–5Sm	1.89	10.15	13.6	2.7
Ni–50Zr	1.28	9.45	15.8	2.1
Ni–45Zr–5Sm	–	–	–	–
Ni–60Zr	1.81	9.72	6.2	3.9
Ni–55Zr–5Sm	–	–	–	–
Ni–70Zr	1.92	10.31	2.9	5.9
Ni–65Zr–5Sm	0.73	3.92	6.2	2.5
3 at% Ni/ZrO_2*	2.20	11.82	0.2	29.0

* Prepared by wet impregnation.

Fig. 10 shows the morphologies by SEM of cross-sections of the Ni–30Zr and Ni–25Zr–5Sm alloy catalysts after reaction. The Ni–30Zr catalyst consists of three layers. EDX analysis reveals that the outer layer is composed mainly of nickel in the metallic state. The thickest intermediate layer consists of metallic nickel and zirconia. The innermost layer is metallic nickel [6]. In the Ni–25Zr–5Sm catalyst, the outer metallic nickel layer is not detected (Fig. 10(b)). The major layer contains nickel, zirconia and samarium oxide, which are uniformly distributed in the layer. Thus, this layer consists of metallic nickel finely dispersed on zirconia containing samarium oxide. Furthermore, this layer contains nanoscale pores [25]. The absence of the outer nickel layer may partly contribute to the enlargement of the surface area.

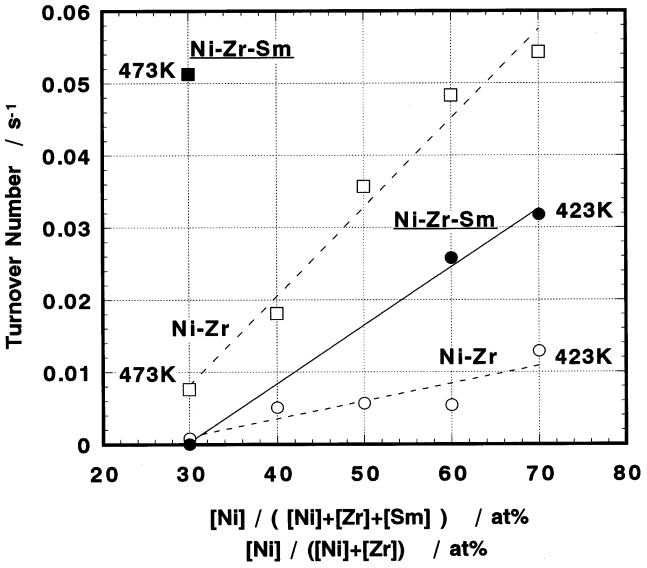

Fig. 9. Change in the turnover number of the catalysts prepared from the amorphous Ni–Zr (open symbols) and Ni–Zr–Sm (solid symbols) alloy precursors as a function of nickel content in the alloy precursors.

4. Conclusions

The catalytic activity for methanation of carbon dioxide was examined for catalysts prepared from amorphous Ni–Zr–Sm and Ni–Zr–Mm alloys and from crystalline Ni–Sm and Ni–Mm alloys and the following conclusions can be drawn:

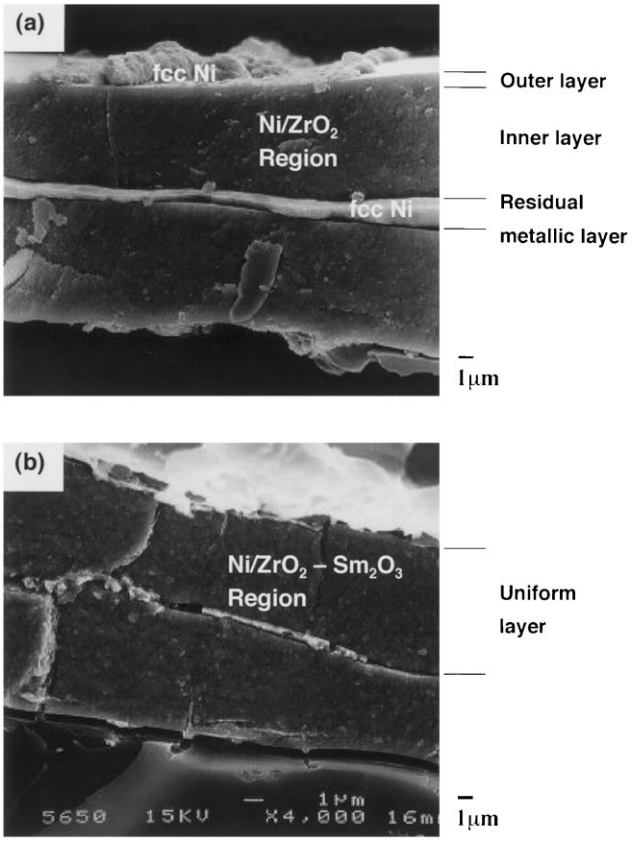

Fig. 10. Scanning electron micrographs of cross-sections of the amorphous Ni–30 at% Zr (a) and Ni–25 at% Zr–5 at% Sm (b) alloy specimens after reaction.

1. The nickel catalysts supported on nano-grained oxides were prepared from amorphous Ni–Zr–Sm and Ni–Zr–Mm alloy and crystalline Ni–Sm and Ni–Mm alloy precursors. These catalysts show higher catalytic activity for methanation of carbon dioxide than a conventionally prepared zirconia supported nickel catalyst prepared by wet impregnation.
2. In the Ni–Zr–5 at% Sm catalysts, an increase in nickel content leads to a gradual increase in the catalytic activity while the samarium-free Ni–Zr catalysts with medium nickel content show the highest conversion.
3. The catalytic activity of nickel supported on tetragonal zirconia is superior to that of nickel supported on monoclinic zirconia, and the stabilization of tetragonal zirconia by the addition of samarium is confirmed for most catalysts except for zirconium-rich samples.
4. Samarium addition stabilizes tetragonal zirconia and increases the number of surface nickel atoms.
5. Activity is enhanced by the addition of 5 at% misch metal only when the catalyst contains 60 at% nickel. The stabilization of tetragonal zirconia was confirmed only for the catalyst containing 60 at% nickel.
6. As for zirconia, samarium oxide and misch metal oxide are regarded as good supports of nickel catalysts for methanation of carbon dioxide. The activity of catalysts for methanation of carbon dioxide decreases in the following order of oxide supports: tetragonal zirconia, misch metal oxides, samarium oxides, monoclinic zirconia.

Acknowledgements

This work is supported in part by the Grant-in-Aid for Scientific Research (A) No. 07405032 and (A) No. 06402051 from the Ministry of Education, Science and Culture. One of the authors (M. Yamasaki) is grateful to the Research Fellowships of the Japan Society for Promotion of Science for Young Scientists No. 1890.

References

[1] T. Inui, T. Takeguchi, Catal. Today 10 (1991) 95.
[2] K. Hashimoto, Kinzoku 93 (1993) 5.
[3] K. Izumiya, E. Akiyama, H. Habazaki, A. Kawashima, K. Asami, K. Hashimoto, N. Kumagai, J. Appl. Electrochem. 27 (1997) 1362.
[4] A. Kawashima, E. Akiyama, H. Habazaki, K. Hashimoto, Mater. Sci. Eng. A226-228 (1997) 905.
[5] H. Habazaki, T. Tada, K. Wakuda, A. Kawashima, K. Asami, K. Hashimoto, in: C.R. Clayton, K. Hashimoto (Eds.), Symposium on Corrosion, Electrochemistry, and Catalysis of Metastable Metals and Intermetallics, The Electrochemical Society, Honolulu, 1993, p. 393.
[6] K. Shimamura, M. Komori, H. Habazaki, T. Yoshida, M. Yamasaki, E. Akiyama, A. Kawashima, K. Asami, K. Hashimoto, Proceedings of the 9th International Conference on Rapidly Quenched and Metastable Materials, 1997, p. 376.
[7] H. Komiyama, A. Yokoyama, H. Inoue, T. Masumoto, H.M. Kimura, Suppl. to Sci. Rep., RITU, A, March 1980, p. 217.
[8] A. Yokoyama, H. Komiyama, H. Inoue, T. Masumoto, H.M. Kimura, Scripta Metall. (1981) 365.
[9] A. Yokoyama, H. Komiyama, H. Inoue, T. Masumoto, H.M. Kimura, J. Chem. Eng. Jpn. 46 (1982) 199.
[10] T. Takahashi, Y. Nishi, T. Kai, in: R.B. Diegle, K. Hashimoto (Eds.), Symposium on Corrosion, Electrochemistry, and Catalysis of Metallic Glasses, The Electrochemical Society, Honolulu, 1988, p. 371.
[11] T. Katona, Z. Hegedus, C. Kopasz, Á. Molnár, M. Bartók, Catal. Lett. 5 (1990) 351.
[12] Á. Molnár, T. Katona, M. Bartók, K. Valga, J. Mol. Catal. 64 (1991) 41.
[13] Á. Molnár, T. Katona, M. Bartók, I.V. Perczel, Z. Hegedus, C. Kopasz, Mater. Sci. Eng. A134 (1991) 1083.
[14] Á. Molnár, T. Katona, M. Bartók, Mater. Sci. Eng. A181/182 (1994) 1095.
[15] T. Katona, Á. Molnár, J. Catal. 153 (1995) 333.
[16] Á. Molnár, L. Domokos, T. Katona, T. Martinek, G. Mulas, G. Coocc, I. Bertóti, J. Szépvölgyi, Mater. Sci. Eng. A226/228 (1997) 1074.
[17] D. Gasser, A. Baiker, Appl. Catal. 48 (1989) 279.
[18] A. Baiker, D. Gasser, J. Chem. Soc. Faraday Trans. 1 (1989) 999.
[19] T. Takahashi, T. Kai, J. Chem. Eng. Jpn. 21 (1995) 961.
[20] R.C. Gravie, J. Phys. Chem. 82 (1978) 218.
[21] R.C. Gravie, J. Phys. Chem. 69 (1965) 1238.
[22] A. Clearfield, Inorg. Chem. 3 (1964) 146.
[23] M. Yamasaki, H. Habazaki, T. Yoshida, M. Komori, K. Shimamura, E. Akiyama, A. Kawashima, K. Asami, K. Hashimoto, Appl. Catal. A Gen. 163 (1997) 187.
[24] M. Yamasaki, H. Habazaki, T. Yoshida, M. Komori, K. Shimamura, E. Akiyama, A. Kawashima, K. Asami, K. Hashimoto, Stud. Surf. Sci. Catal. 114 (1998) 451.
[25] H. Habazaki, T. Yoshida, M. Yamasaki, M. Komori, K. Shimamura, E. Akiyama, A. Kawashima, K. Hashimoto, Stud. Surf. Sci. Catal. 114 (1998) 261.
[26] R.J. Farrauto, AIChE Symp. Ser. 70 (1975) 9.
[27] J. Barrault, A. Chafik, Appl. Catal. 67 (1991) 257.